

Optical properties of two-dimensional negative-phase-velocity-medium photonic crystals

Yong Zeng,^{1,2} Ying Fu,^{1,*} Xiaoshuang Chen,^{2,†} Wei Lu,^{2,‡} and Hans Ågren¹

¹*Department of Theoretical Chemistry, Royal Institute of Technology, S-106 91 Stockholm, Sweden*

²*National Laboratory for Infrared Physics, Shanghai Institute of Technical Physics, Chinese Academy of Science, 200083 Shanghai, China*

(Received 5 April 2006; published 29 June 2006)

By an extended plane-wave-based transfer-matrix method, the photonic band structure and the corresponding transmission spectrum have been calculated for a two-dimensional photonic crystal composed of negative-phase-velocity-medium (NPVM) cylindrical rods. Dispersionless anticrossing bands in the two-dimensional NPVM periodic structure are generated by the couplings among surface polaritons localized in the NPVM rods. In part of the negative-phase-velocity frequency region, the photonic band structures of the NPVM photonic crystal are characterized by a topographical continuous dispersion relationship accompanied by many anticrossing bands. The effect of the filling fraction of the NPVM rods on the optical properties of photonic crystals has also been studied.

DOI: [10.1103/PhysRevE.73.066625](https://doi.org/10.1103/PhysRevE.73.066625)

PACS number(s): 42.70.Qs, 41.20.Jb

Starting from the pioneering work of Yablonovich [1] and John [2] in 1987, the past decades have witnessed an extended development in photonic crystals (PCs), also known as photonic band gap (PBG) materials. The dielectric constituents of these materials are periodically arranged in space, in one, two, or three dimensions, with important applications in the optical, microwave, and infrared fields [3]. One of their important properties is to mold and control the flow and distribution of the light at the microscopic level. In PCs, the synergistic interplay between the microcavity resonance within each constituent and the Bragg scattering resonance among constituents leads to the formation of a PBG, within which no propagating electromagnetic (EM) modes are allowed. The photonic density of states in PCs is suppressed in the PBG [4]. This feature opens the possibility for many technical applications including lossless PC waveguides, low-threshold PC lasers, and high- Q PC nanocavities [3].

Early research was largely concentrated on PBG materials consisting of positive and frequency-independent dielectrics. In the past few years, negative-phase-velocity (NPV) media [5–7], also named left-handed materials and negative-refractive-index media, have been successfully fabricated [8,9]. This new type of metamaterial was first discussed by Veselago in 1968, characterized simultaneously by a negative permittivity and a negative permeability and therefore a negative refractive index in certain frequency ranges [10]. For an EM plane wave propagating in such a medium, the electric field, the magnetic field, and the wave vector form a left-handed system; therefore, the Poynting vector lies in the direction opposite to that of the wave vector. Many anomalous effects can exist in these metamaterials such as a reversed Doppler shift, reversed Cerenkov radiation, negative radiation pressure, and an inverse Snell-Descartes law. Recently, a periodic arrangement of NPV materials, namely,

NPV-medium photonic crystals, has become the object of intense experimental and theoretical interest [11–15]. Like polaritonic PCs whose μ is homogeneous while ϵ is frequency dependent [16,17], the application of NPV materials in PCs is expected to introduce a whole range of exciting physical phenomena. For instance, a multilayer structure with stacking alternating layers of ordinary (positive- n) and NPV materials can result in an omnidirectional zero- \bar{n} gap [12,13], where the defect modes depend weakly on the incident angles [18].

In general, the permittivity and permeability of a NPV material are frequency dependent [11]. In a split ring resonator used to create negative magnetic materials, the permeability is normally expressed as $\mu(\omega) = 1 - \omega_m^2 / \omega(\omega + i\gamma)$, where ω_m is the effective magnetic plasma frequency, ω is the frequency of the light, and γ represents the light absorption [11]. Due to these dispersive properties of NPV materials, the study of high-dimensional NPV-medium PCs thus becomes rather complicated for many conventional theoretical methods, such as the plane-wave expansion method [3] and the finite-difference time-domain method [19].

In this work we use an extended plane-wave-based transfer-matrix method [20] to study the optical properties of a two-dimensional (2D) NPV-material PC. The 2D PC considered here is a square lattice of NPV-material cylindrical rods embedded in air background. The rods are aligned along the x axis and positioned periodically in the yz plane. The physical background of our method is as follows. (1) Divide the whole PC structure into thin slices along the z -axis direction; within each slice ϵ and μ are approximated as z independent (they are however y dependent). (2) It is assumed that each slice is surrounded by two thin air films with zero thickness. (3) Express the EM field in the air films by Floquet harmonics. (4) Express the EM field in each slice by the eigenmodes in the slice. (5) Use the boundary conditions between EM fields in the slice and two neighboring air films to obtain the transfer matrix or the scattering matrix. (6) Use the obtained matrix to calculate the transmission spectrum of the PC. The photonic band structure of the PC can thus be obtained by using Bloch's theorem. Since the independent

*Electronic address: fyg@theochem.kth.se

†Electronic address: xschen@mail.sitp.ac.cn

‡Electronic address: luwei@mail.sitp.ac.cn

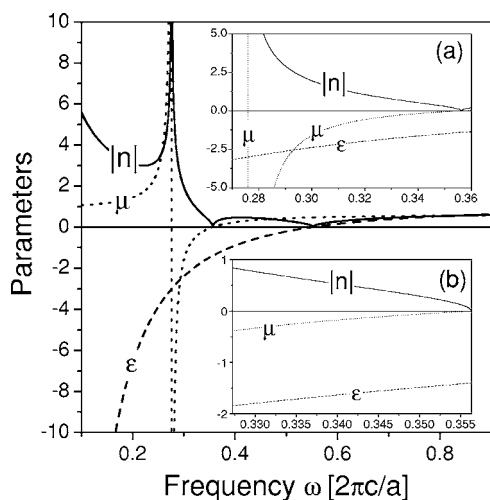


FIG. 1. $\mu(\omega)$, $\epsilon(\omega)$, and $|n(\omega)|$ of the NPV-material cylindrical rods as functions of ω .

variable in these calculations is the frequency rather than the wave vector, it can therefore effectively simulate dispersive PCs; even though their permeability and permittivity are frequency dependent and negative.

Based on this approach, the photonic band structures and the corresponding spectra of 2D NPV-material PCs are calculated. For the sake of easy comparison, the relative permittivity $\epsilon(\omega)$ and relative permeability $\mu(\omega)$ of the rods are adopted from Ref. [21]. The free electron representation of $\epsilon(\omega)$ is assumed,

$$\epsilon(\omega) = 1 - \frac{\omega_p^2}{\omega^2}, \quad (1)$$

where ω_p is the frequency of bulk longitudinal electron excitations, and

$$\mu(\omega) = 1 - \frac{F\omega^2}{\omega^2 - \omega_0^2}. \quad (2)$$

The parameters assumed here are $F=0.4$, $\omega_p=0.552(2\pi c/a)$, $\omega_0=0.276(2\pi c/a)$, and the radius of the rod $r=0.3a$, where a is the lattice constant and c is the speed of light in vacuum. Notice that ω_0 and ω_p used here are 1/20 of those used in Ref. [21]. Dissipative properties of NPV materials are neglected in Eqs. (1) and (2), which is valid if the light absorption is very small. Moreover the small light absorption has a very limited effect on the band structure.

Figure 1 shows $\mu(\omega)$, $\epsilon(\omega)$, and $|n(\omega)|$ of the NPV-material cylindrical rods as functions of ω . For frequencies $\omega < \omega_0$, $\epsilon(\omega) < 0$ and $\mu(\omega) > 0$, i.e., the metamaterial is singly negative; for $\omega_0 < \omega < 0.35635(2\pi c/a)$, both $\mu(\omega)$ and $\epsilon(\omega)$ are negative so that the metamaterial is left handed; for $0.35635(2\pi c/a) < \omega < \omega_p$, $\epsilon(\omega) < 0$ and $\mu(\omega) > 0$, and the metamaterial is again singly negative; for $\omega > \omega_p$, both $\mu(\omega)$ and $\epsilon(\omega)$ are positive, and the metamaterial is right handed. Notice that $0.35635 = \omega_b/20$ used in Ref. [21].

The photonic band structures for the transverse magnetic mode along the Γ -X direction are calculated and shown in Fig. 2, and the corresponding transmission spectrum along

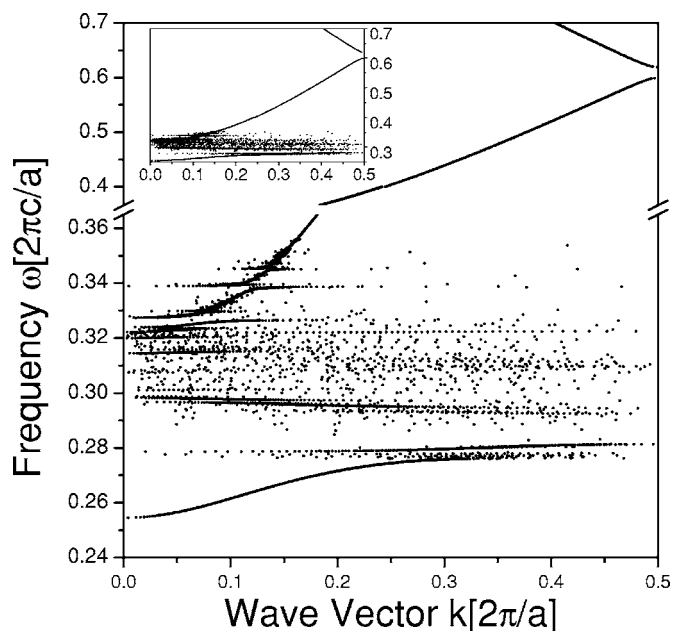


FIG. 2. The photonic band structure of a two-dimensional PC. The inset shows the unbroken band structures. The increment frequency here is $1.0 \times 10^{-6}(2\pi c/a)$. Notice that more accurate results can be obtained by decreasing the frequency increment.

the same direction for a 16-layer structure is also calculated and shown in Fig. 3(a). Two profound similarities between our periodic structure and the single rod are observed by comparing Fig. 3(a) with the scattering resonances of a single NPV-material cylindrical rod shown in Fig. 2(b) of Ref. [21].

(1) Anticrossing bands appear when the metamaterial is NPV (see the inset of Fig. 4 as an example), which are sepa-

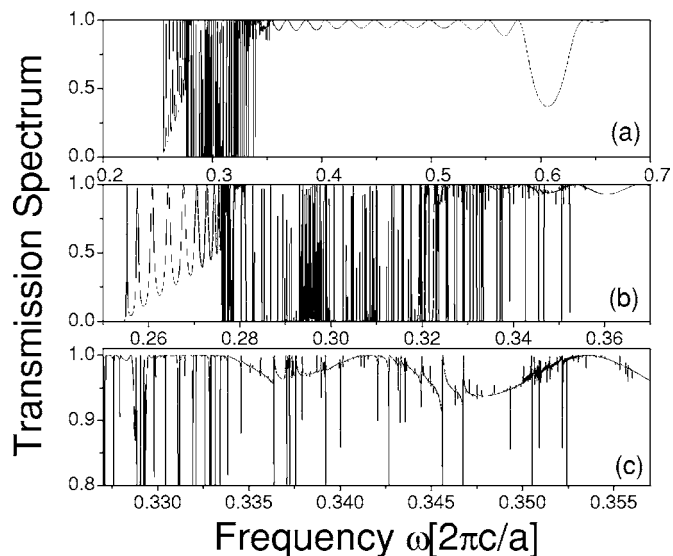


FIG. 3. Transmission spectrum of the two-dimensional PC. The frequency range is (a) $[0.2(2\pi c/a), 0.7(2\pi c/a)]$, (b) $[0.25(2\pi c/a), 0.37(2\pi c/a)]$, and (c) $[0.327(2\pi c/a), 0.357(2\pi c/a)]$. Notice that more accurate results can be obtained by decreasing the frequency increment.

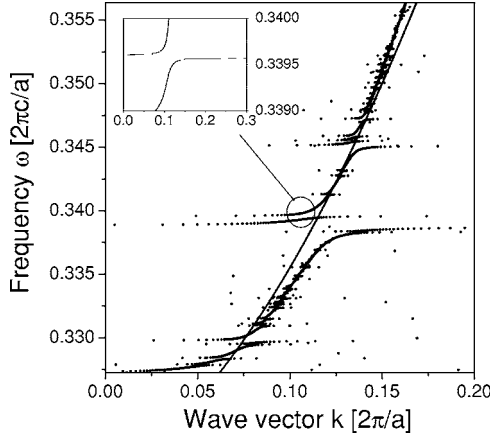


FIG. 4. The dispersion curves of the two-dimensional negative-phase-velocity-medium PC (dotted) and the corresponding effective structure (solid line). The inset shows the anticrossing bands around $0.340a/2\pi c$.

rated by very narrow band gaps and are almost dispersionless around the band edges. Moreover, the dispersionless bands (in other words, their group velocities are almost zero) lead to sharp resonant peaks in the transmission spectrum. Similar results were reported in the scattering resonances of the single NPV-material rod [21], where resonances also exist in the NPV frequency region. We interpret this observation by collective couplings among highly localized resonance modes, surface polaritons, of the NPV-material rods [21,22]. It is noticed that the anticrossing bands also appear in polaritonic PCs [16].

(2) A narrow band gap exists slightly above $0.6(2\pi c/a)$, corresponding to the valley in the transmission spectrum of Fig. 3(a). A similar dip was also found around the same place in the scattering resonances of a single rod [21]. This is a direct result of the fact that the refractive index of the cylindrical rod around $0.6(2\pi c/a)$ is 0.275, and the volume-averaged refractive index of the whole structure, roughly given by

$$\bar{n}(\omega) = [\pi r^2 \sqrt{\epsilon(\omega)\mu(\omega)} + (a^2 - \pi r^2) \times 1.0]/a^2, \quad (3)$$

becomes only 0.8. This value is very close to the refractive index of vacuum, so that the transmission rates around this narrow band gap are nonzero. They are about 37%, as shown in Fig. 3(a).

From these two similarities, it can be concluded that, as in a polaritonic PC, the band structure of a high-dimensional NPV-material PC is governed principally by the surface polaritons localized in individual rods, whose frequencies are determined by the rods' geometries. The periodicity of the rods in the PC introduces only weak dispersion [16].

Furthermore, a wide band gap, from zero to $0.2545(2\pi c/a)$, is shown in Figs. 2 and 3(a), which is mainly due to the single-negative property of the metamaterial, so that EM waves decay quickly when propagating through this structure and only evanescent waves are allowed. As shown in Figs. 2 and 3(b), a continual dispersion curve exists in the frequency region $[0.2545(2\pi c/a), \omega_0]$, where $\epsilon(\omega)$ is close

to zero and $\mu(\omega) > 0$. Similar dispersion curves were reported in 2D polaritonic PCs since the metamaterials in this frequency region have the same optical properties as the polaritonic materials [16].

From $0.32728(2\pi c/a)$ to $0.35635(2\pi c/a)$ where the metamaterials are NPV, the dispersion relationship can be topographically described as continual, accompanied by anticrossing bands. The dispersion relation here has the same physical origin as that in $[0.35635(2\pi c/a), \omega_p]$, where the metamaterial is singly-negative with a negative $\epsilon(\omega)$ and a positive $\mu(\omega)$. Direct evidence can be found from the complete band structure shown in the inset of Fig. 2, where the dispersion curve is continuous from $0.32728(2\pi c/a)$ to ω_p . This phenomenon can also be explained by the long-wavelength approximation, that is, when the wavelength of the propagating EM wave is much longer than the lattice constant of the PC, the dispersion relationship becomes approximately linear, and the PC is effectively homogeneous. Notice that the refractive index of the NPV material in this region is very close to zero, as shown in Fig. 1(b). In order to explain it more clearly, we plot the dispersion relationship of the effectively homogeneous structure in Fig. 4. More explicitly, the effective refractive index of the whole structure used here can be approximated by

$$\bar{n}(\omega) = [-\pi r^2 \sqrt{\epsilon(\omega)\mu(\omega)} + (a^2 - \pi r^2) \times 1.0]/a^2, \quad (4)$$

and the corresponding dispersion relationship, the thick solid line in Fig. 4, is obtained from $k = \bar{n}(\omega)\omega/c$. Notice that the solid line is shifted upward by $0.0258(2\pi c/a)$ in order to demonstrate that the two curves have similar slopes, i.e., there are almost identical speeds of the energy propagation (given by $d\omega/dk$) in the effective structure and in the periodic structure. Notice that Eq. (4) is very different from Eq. (3). The refractive index obtained by Eq. (4) can be zero or even negative because of the negative refractive index of the NPV material, whereas Eq. (3) only gives a positive value for the index.

When the volume-averaged refractive index of a multilayer structure $\bar{n} = \int_0^a n(x)dx/a$ equals zero, where a is the lattice constant, a band gap, namely a zero- \bar{n} gap, will appear in the band structure of the one-dimensional structure for normal incidence [12]. Our 2D sample also has a similar zero- \bar{n} gap around $\omega a/2\pi c = 0.293125$ shown in Fig. 5. When the refractive index of the cylindrical rods around this frequency is about -2.5368 , the averaged refractive index of the 2D PC is zero by Eq. (4). In the 2D PC case, the zero- \bar{n} gap is only one of many minigaps induced by the anticrossing interaction. It is very important to point out the concept of nihility, where the NPV material annihilates the surrounding normal material; therefore, a more accurate description of a NPV material is negative space [6,23].

Moreover, a very sharp peak with very narrow bandwidth is shown at $0.29307275(2\pi c/a)$ in Fig. 5, and the ratio between the full width at half maximum and the peak frequency is extremely small (only 6.8×10^{-8}). This property can be used to design narrowband filters.

In order to study the filling effect on the optical properties of a 2D NPV-material PC, the transmission spectrum of a

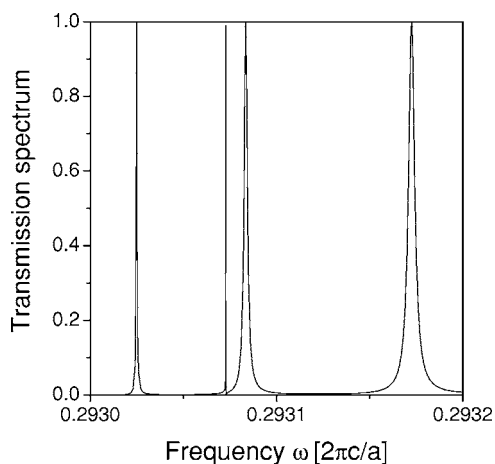


FIG. 5. Transmission spectrum of the two-dimensional PC around $\omega a/2\pi c=0.293125$.

similar structure is calculated, where only the radius r of the rods is significantly reduced to $0.05a$ (corresponding to a filling factor as small as 0.785%). The result is shown in Fig. 6(a), and the transmission spectrum of $r=0.3a$ is also plotted in Fig. 6(b) for direct comparison. Clearly, the transmission coefficients in Fig. 6(a) are all 100% except a few discrete frequencies. It is a consequence of two factors. (1) The filling fraction of the NPV-material rods is so small that the Bragg scattering resonances in such a PC are very weak, and the periodic arrangement of these rods hardly affects the dispersion relation of this structure, and thus the light propagates easily through the structure. (2) The distance between the surface polaritons localized in the neighboring rods increases when the radius of the rod is decreased, resulting in a weaker coupling among the surface polaritons. Therefore, only those polaritons whose energy propagation length is long enough can significantly reflect the incident light [24]. This is the reason for the limited number of transmission valleys in Fig. 6(a), as compared with Fig. 6(b).

In a brief summary, we have studied the photonic band structure and the corresponding transmission spectrum of a two-dimensional negative-phase-velocity-medium (NPVM) photonic crystal by an extended plane-wave-based transfer-matrix method. From the detailed comparisons between the

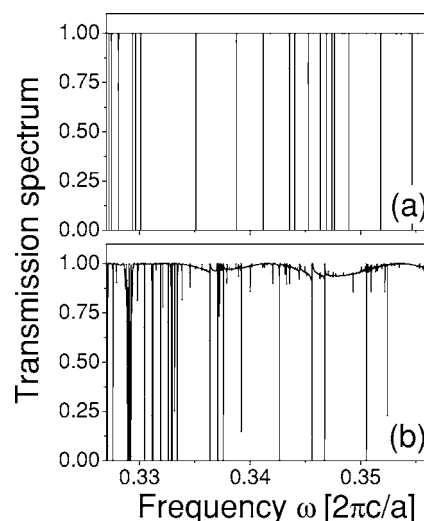


FIG. 6. Transmission spectrum for the transverse magnetic mode along the Γ -X direction of a 16-layer two-dimensional PC. The radius of the rods is (a) $0.05a$ (b) $0.3a$. Notice that more accurate results can be obtained by decreasing the frequency increment.

periodic structure and a single NPVM cylindrical rod, it has been shown that due to the coupling among the surface polaritons localized in neighboring NPVM rods, many anticrossing bands exist in the NPVM periodic structure. Moreover, a topographical continual dispersion relation is found in a part of the negative-phase-velocity frequency region, accompanied by many anticrossing bands, which has been explained by the long-wavelength approximation. The effect of the filling fraction of the NPVM rods on the optical properties of photonic crystals is also studied.

We thank Jun Jiang of Royal Institute of Technology for his invaluable help. This work is supported by the Swedish Foundation for Strategic Research (SSF), as well as by the Chinese National Key Research Special Fund, the Chinese National Science Foundation (Grants No. 60576068 and No. 60476040), the Grand Fund of Chinese National Science Foundation (Grant No. 10234040), and the Key Fund of the Shanghai Science and Technology Foundation (Grant No. 05DJ14003).

-
- [1] E. Yablonovitch, *Phys. Rev. Lett.* **58**, 2059 (1987).
 [2] S. John, *Phys. Rev. Lett.* **58**, 2486 (1987).
 [3] K. Sakoda, *Optical Properties of Photonic Crystals* (Springer, Berlin, 2001).
 [4] Y. Zeng, X. Chen, and W. Lu, *Phys. Rev. E* **70**, 047601 (2004).
 [5] J. B. Pendry, *Phys. Rev. Lett.* **85**, 3966 (2000).
 [6] D. R. Smith, J. B. Pendry, and M. C. K. Wiltshire, *Science* **305**, 788 (2004).
 [7] A. Lai, C. Caloz, and T. Itoh, *IEEE Microw. Mag.* **5**, 34 (2004).
 [8] D. R. Smith, W. J. Padilla, D. C. Vier, S. C. Nemat-Nasser, and S. Schultz, *Phys. Rev. Lett.* **84**, 4184 (2000).
 [9] R. A. Shelby, D. R. Smith, and S. Schultz, *Science* **292**, 77 (2001).
 [10] V. G. Veselago, *Sov. Phys. Usp.* **10**, 509 (1968).
 [11] S. A. Ramakrishna, *Rep. Prog. Phys.* **68**, 449 (2005).
 [12] J. Li, L. Zhou, C. T. Chan, and P. Sheng, *Phys. Rev. Lett.* **90**, 083901 (2003).
 [13] I. V. Shadrivov, A. A. Sukhorukov, and Y. S. Kivshar, *Phys. Rev. Lett.* **95**, 193903 (2005).
 [14] L. Feng, X. Liu, Y. Tang, Y. Chen, J. Zi, S. Zhu, and Y. Zhu, *Phys. Rev. B* **71**, 195106 (2005).
 [15] L. Chen, S. He, and L. Shen, *Phys. Rev. Lett.* **92**, 107404 (2004).

- [16] K. C. Huang, P. Bienstman, J. D. Joannopoulos, K. A. Nelson, and S. Fan, *Phys. Rev. B* **68**, 075209 (2003).
- [17] Y. Zeng, X. Chen, and W. Lu, *Phys. Lett. A* **351**, 319 (2006).
- [18] H. Jiang, H. Chen, H. Li, Y. Zhang, and S. Zhu, *Appl. Phys. Lett.* **83**, 5386 (2003).
- [19] A. Taflove, *Computational Electrodynamics: The Finite-Difference Time-Domain Method* (Artech house, Boston, 1995).
- [20] Y. Zeng, Y. Fu, X. Chen, W. Lu, and H. Ågren (unpublished).
- [21] S. Ancey, Y. Décanini, A. Folacci, and P. Gabrielli, *Phys. Rev. B* **72**, 085458 (2005).
- [22] R. Ruppin, *Solid State Commun.* **116**, 411 (2000).
- [23] A. Lakhtakia, *Int. J. Infrared Millim. Waves* **3**, 339 (2002).
- [24] A. V. Zayats, I. I. Smolyaninov, and A. A. Maradudin, *Phys. Rep.* **408**, 131 (2005).